Magnetism of the endohedral metallofullerenes $M@C_{82}$ (M=Gd,Dy) and the corresponding nanoscale peapods: Synchrotron soft x-ray magnetic circular dichroism and density-functional theory calculations

R. Kitaura, H. Okimoto, and H. Shinohara*
Department of Chemistry and Institute for Advanced Research, Nagoya University, Nagoya 464-8602, Japan

T. Nakamura and H. Osawa
Japan Synchrotron Radiation Research Institute, SPring-8, Sayo, Hyogo 679-5198, Japan
(Received 8 June 2007; revised manuscript received 4 August 2007; published 28 November 2007)

Synchrotron soft x-ray magnetic circular dichroism (SXMCD) spectroscopy at the Gd and Dy M_5 edges is reported on endohedral metallofullerenes ($M@C_{82}$, M=Gd and Dy) and the corresponding nanopeapods [$(M@C_{82})@$SWNT, SWNT represents single wall carbon nanotube] in a temperature range between 10 and 40 K. The magnetic moment has also been determined by theoretical calculations, which are based on the Hartree-Fock approximation with relativistic corrections. Because of the element-specific measurement of SXMCD, magnetization processes of Gd and Dy ions of nanopeapods have been selectively observed. The temperature dependence of magnetic moments of the metallofullerenes and nanopeapods follows the Curie-Weiss law with a small Weiss temperature, indicating that the magnetic interaction between encapsulated rare-earth metal atoms is relatively weak. Although the observed differences in Curie constants and Weiss temperatures between $Gd@C_{82}$ and $(Gd@C_{82})@$SWNT are small, those of $Dy@C_{82}$ and $(Dy@C_{82})@$SWNT are significant. This observation is consistently explained by charge transfer-induced crystal-field effects.

DOI: 10.1103/PhysRevB.76.172409 PACS number(s): 75.75.+a, 71.20.Tx, 73.22.−f, 78.70.Dm

Endohedral metallofullerenes[1] and nanopeapods[2–4] have attracted much attention during the past decade and added a new dimension to materials-directed physics and chemistry; properties and applications of these materials range from magnetism, photoluminescence, transport and mechanical properties, molecular switches, field effect transistors, and drug deliveries.[5–13] In the so-called nanopeapods, metallofullerene molecules align in regulated one-dimensional fashion in single wall carbon nanotubes (SWNTs) with short intermolecular and molecular-tube wall distances, which has been known to enhance fullerene-tube and fullerene-fullerene interactions such as charge transfer, orbital hybridization, and exchange interaction. In fact, low-temperature scanning tunneling microscopy and spectroscopy studies have revealed that the band gap of $(Gd@C_{82})@$SWNT is significantly modulated along the tube axis and the original band gap of the SWNT (0.43 eV) is reduced to 0.17 eV where the fullerenes are expected to be located due to the local strain and charge transfer from encapsulated $Gd@C_{82}$ molecules.[14] These unique geometrical and electronic structures should affect the magnetic properties of encapsulated metal atoms and are expected to be the origin of specific magnetic properties arising from low dimensionality.

While several studies on magnetic properties of metallofullerenes have been performed recently,[5,15–17] no investigation has so far been done on nanopeapods. One of the main reasons of this is that a nanopeapod sample usually contains a large amount of ferromagnetic impurities (sometimes more than 10 wt %) such as Co and Ni particles that originates from catalyst metals required for the synthesis of SWNTs. Unfortunately, these ferromagnetic impurities have precluded the investigation of magnetic properties of nanopeapods using superconducting quantum interference device magnetometry. This difficulty can, however, be overcome by incorporating the so-called element selective magnetization measurements using soft x-ray magnetic circular dichroism (SXMCD). Because the energy of M edges of rare-earth metal atoms such as Gd and Dy is apart from L edges of Ni and Co, we are able to selectively observe a magnetization of rare-earth metal atoms without any disturbance from the impurities. Furthermore, we can take advantages of synchrotron radiation x-ray source. Synchrotron radiation is a very high brilliance soft x-ray source, which enables us to deal with a quite small amount of sample materials. This is a significant advantage considering a time-consuming process of synthesis, extraction, and purification of endohedral metallofullerenes and the corresponding synthesis of nanopeapods.

Synchrotron SXMCD is, therefore, one of the most powerful techniques to investigate magnetic properties of nanopeapods encapsulating metallofullerenes. Here, we report the results of SXMCD measurements on $Gd@C_{82}$, $Dy@C_{82}$, $(Gd@C_{82})@$SWNT, and $(Dy@C_{82})@$SWNT, and discuss a local magnetization of these materials resulting from the encapsulated Gd and Dy atoms. Metallofullerenes, $Dy@C_{82}(C_{2v})$ and $Gd@C_{82}(C_{2v})$, were synthesized by arc discharge and were purified by multistep high performance liquid chromatography. A filling of the metallofullerenes in SWNTs was performed by the gas phase reaction method already reported,[18] and the filling was confirmed by high-resolution transmission electron microscope (HRTEM) observations. Figure 1 shows a HRTEM image of $(Gd@C_{82})@$SWNT, for example. SXMCD measurements were performed at the twin-helical-undulators soft x-ray beamline, BL25SU in SPring-8 using a MCD spectrometer equipped with an electromagnet of 1.9 T. Absorption intensities were recorded by the total electron yield method applying a bias voltage of 36 V to samples. Prior to the SXMCD measurement, a sample was heated at 400 K in an

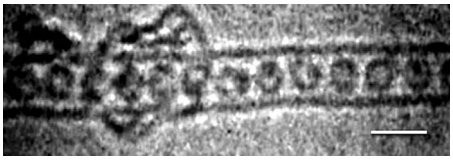

FIG. 1. A HRTEM image of $(Gd@C_{82})@SWNT$. The scale bar is approximately 2 nm.

ultra-high-vacuum chamber to remove solvent and adsorbed molecules. The amount of samples used in each SXMCD measurement was less than 100 μg.

First, we show a result of electronic structure calculations of $Dy@C_{82}$, which was performed by the density-functional theory. The calculation was carried out with the GAUSSIAN03 program package using B3LYP functional, CREMBL effective core potential for the Dy atom and 6-31G* basis set for C atoms. Figure 2 show the calculated equicontour (1.3 $e/Å^3$) spin density map of $Dy@C_{82}$. As clearly illustrated in Fig. 2, a spin density resides not only on an encapsulated Dy atom but also on a C_{82} cage. Encapsulated Dy atoms are thus able to interact with neighboring Dy atoms through encapsulating C_{82} cages. The Mulliken electron density and the spin density on Dy are +3.06 and 5.07, respectively. This value is consistent with $4f^9$ electron configuration, suggesting that three electrons are transferred from the encapsulated Dy to C_{82} cage, i.e., $Dy^{3+}@C_{82}^{3-}$. A similar calculation result has been obtained for $Gd@C_{82}$, which shows encapsulated Gd is also in a trivalent state. The trivalency of the Gd atoms in a $Gd@C_{82}$ metallofullerene has also been reported by Suenaga *et al.* based on electron-energy-loss measurements.[19] The calculated trivalency of $Dy@C_{82}$ is consistent with a previous x-ray absorption (XAS) study.[20]

Figure 3 shows the observed and calculated (normalized) XAS and the corresponding SXMCD spectra of the Gd and Dy M_5 edges on $Gd@C_{82}$ and $Dy@C_{82}$ and their corresponding nanopeapods at 10 K and 1.9 T. In spite of a little

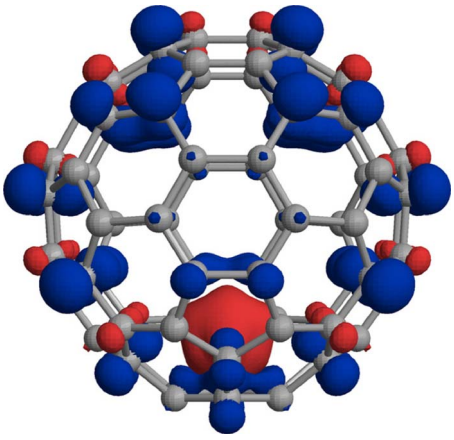

FIG. 2. (Color online) Optimized structure of $Dy@C_{82}$ together with spin density distribution that is shown as contour of equidensity (1.3 $e/Å^3$). The isodensity surface is defined by difference between α and β spin where red and blue surfaces represent a plus and minus spin density region, respectively.

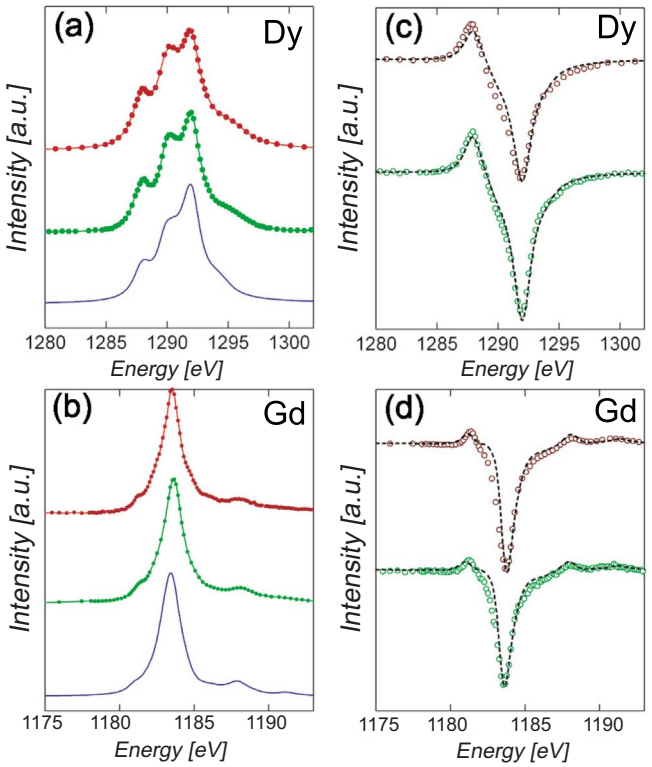

FIG. 3. (Color online) Theoretical and observed isotropic XAS and SXMCD spectra of $Dy@C_{82}$, $(Dy@C_{82})@SWNT$, $Gd@C_{82}$, and $(Gd@C_{82})@SWNT$. [(a) and (b)] Theoretical XAS spectra (solid line), and observed XAS spectra of metallofullerenes (upper solid circle) and nanopeapods (lower solid circle). [(c) and (d)] Theoretical SXMCD spectra (dotted line), and observed SXMCD spectra of metallofullerenes (upper open circle) and nanopeapods (lower open circle).

amount of the samples used in these measurements, the observed XAS and SXMCD spectra exhibit sufficient signal-to-noise ratios. The spectra show a multiplet structure due to electric dipole transitions from the $3d$ core level to the unoccupied $4f$ levels. The difference of XAS and SXMCD spectral features between metallofullerenes and the corresponding nanopeapods is very small, which represents electronic states, such as charge state, of encapsulated Gd and Dy ions are nearly the same.

To obtain the magnetic moments, the spectral simulation has been performed by using Cowan's atomic Hartree-Fock (HF) program with relativistic corrections.[21] In this simulation, we have assumed that Gd and Dy are in trivalent states and, thus, the ground and excited electronic configurations are represented as $3d^{10}4f^n$ and $3d^94f^{n+1}$, respectively, where n values are 7 for Gd and 9 for Dy. The electrostatic and exchange parameters are all scaled down to 73% of their HF values, and the peak shape has been modeled by Fano functions with an appropriate full width at half maximum to reproduce the observed spectra. As illustrated in Fig. 3, the agreement between experimental and theoretical spectra is very well in all cases. This also confirms the trivalent state of the encapsulated Dy and Gd atoms studied here, which is consistent with the theoretical calculations and the previous experimental results.

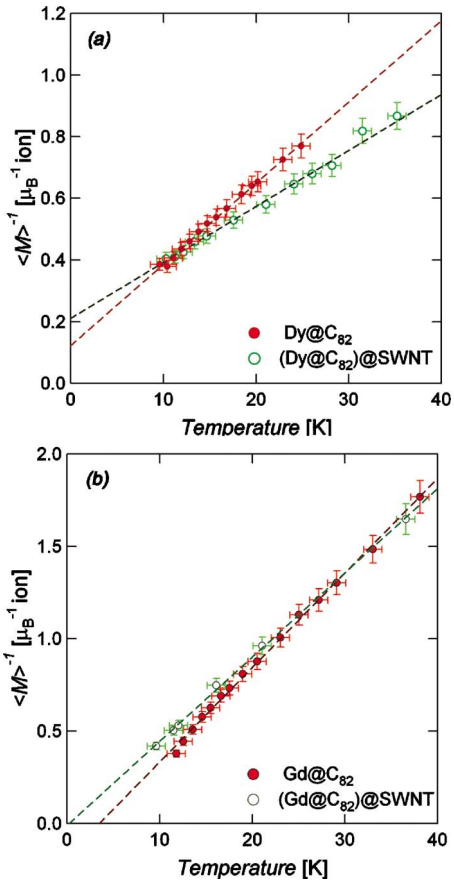

FIG. 4. (Color online) Plots of reciprocal magnetization in external magnetic field $B=1.9T$. (a) Plot of Dy@C_{82} and (Dy@C_{82})@SWNT, and (b) plot of Gd@C_{82} and (Gd@C_{82})@SWNT. The dotted line represents fitting results by the Curie-Weiss law.

The present spectral simulation can also provide a magnetization of the encapsulated metal ions. For example, magnetization of Dy ions in Dy@C_{82} is 2.48 μ_B at 10 K and 1.9 T. The temperature dependences of the SXMCD spectra between 10 and 50 K do not show any change of the line shape, but show a monotonic decrease of its intensity; the local magnetic moments of the encapsulated rare-earth ions decrease as the temperature increases. By obtaining magnetization of the encapsulated metal atoms at each temperature, we can plot the reciprocal magnetization against temperature, which is shown in Fig. 4.

As clearly seen in Fig. 4, all of the reciprocal magnetization shown in the figure is proportional to temperature, which are well fitted by the Curie-Weiss law. The obtained Curie constants, Weiss temperatures, and effective magnetic moments are listed in Table I. The effective magnetic moments and Weiss temperatures of Gd@C_{82} and Dy@C_{82} are reduced compared to free trivalent ions, which is consistent with previous reports[16,17] [10.7 μB for free Dy^{3+} ($^6H_{15/2}$) and 7.9 μ_B free Gd^{3+} ($^8S_8$)]. Two causes can be responsible for reduction of the magnetic moment: (1) a crystal-field splitting (due to the presence of the carbon cage) of the metal orbital momentum states and (2) a hybridization of the 4f orbitals of encapsulated metal atoms with the carbon cage π orbitals, resulting in an electron backdonation between cage and encapsulated metals. At present, we are not certain as to which factor is dominant for the observed reduction of the magnetic moment in the Dy@C_{82} case. However, in Gd@C_{82}, the crystal-field effect cannot explain the reduction because the ground state of Gd^{3+} ion is $^8S_8$ with $\langle L_z \rangle = 0$. This small moment reduction (10%) should, therefore, be caused by orbital hybridization effect between the 4f orbital of Gd and p orbitals of the carbon cage.

TABLE I. Obtained Curie constants and Weiss temperatures of metallofullerenes and corresponding nanopeapods.

Compounds	C (μ_B K)	Θ (K)	μ_{eff} (μ_B)
Dy@C_{82}	38.0±3.5	−4.6±1.5	9.5±0.4
Gd@C_{82}	19.6±1.4	3.5±0.9	6.8±0.5
(Dy@C_{82})SWNT	55.3±4.0	−11.6±1.3	11.4±0.4
(Gd@C_{82})SWNT	22.0±1.7	0.2±1.1	7.2±0.3

As clearly seen in Fig. 4(b), the temperature dependence of magnetization of Gd@C_{82} and the corresponding nanopeapods are similar, resulting in similar Weiss temperature and effective magnetic moments. This means that the encapsulation of Gd@C_{82} by SWNTs does not significantly affect magnetic interaction between Gd ions and their 4f magnetic moments. In contrast, as shown in Fig. 4(a), the reciprocal magnetization plot of Dy@C_{82} differs significantly from that of (Dy@C_{82})@SWNT, which leads to a different Weiss temperature and effective magnetic moments. The absolute value of the Weiss temperature of (Dy@C_{82})@SWNT is higher than that of Dy@C_{82}, which exhibits that antiferromagnetic interaction between Dy ions is enhanced in (Dy@C_{82})@SWNT compared to that in Dy@C_{82}.

A probable reason for the enhancement is a shortening of the intermolecular distances of Dy@C_{82} from bulk crystals to the nanopeapods. Our preliminary x-ray diffraction measurements reveal that a distance between the nearest neighbor molecule in nanopeapods is much shorter than that in bulk crystal; the nearest neighbor distances are ~1.12 and 1.05 nm for bulk crystals of Dy@C_{82} and the corresponding nanopeapods, respectively. The observed short intermolecular distance probably enhances the antiferromagnetic interaction between Dy ions encapsulated in neighboring fullerene cages.

While the effective magnetic moment of Gd ion of Gd@C_{82} is similar to that of (Gd@C_{82})@SWNT, the effective magnetic moment of Dy ion of Dy@C_{82} is 17% as small as that of (Dy@C_{82})@SWNT. As in the effect of encapsulation of Dy ions by C_{82} cages, the encapsulation of Dy@C_{82} by SWNTs produces a crystal field and an orbital hybridization. As discussed above, the change of magnetization behavior in Gd^{3+} ($^8S_8$) should be attributed to orbital hybridization between a 4f orbital and p orbitals of a C_{82} cage; the encapsulation of Gd@C_{82} by SWNTs does not substantially affect the orbital hybridization. Therefore, we conclude that the magnetic moment change is caused by a crystal-field splitting resulting from C_{82} carbon cages. Previous theoretical calculations on (La@C_{82})@SWNT suggest that a charge

transfer occurs from SWNTs p orbital to encapsulated $La@C_{82}$ molecules when $La@C_{82}$ molecules are encapsulated by SWNTs.[22] This charge transfer from SWNTs to fullerene cages causes a change of electron density on C_{82} cages. As a result of this charge transfer, electric field acting on encapsulated Dy atoms concomitantly changes in $(Dy@C_{82})@SWNT$, which leads to different crystal-field splitting of the Dy ions. At the low temperature employed in the present study, even a relatively small crystal-field splitting (i.e., several meV) can provide significant magnetic moment change, because the properties of an electronic state are almost determined by the lowest energy splitting by the crystal-field in the low temperature. The change of magnetization behavior of Dy^{3+} ion may originate from the change of crystal-field splitting caused by charge transfers from SWNTs to $Dy@C_{82}$ metallofullerenes.

In conclusion, we have applied SXMCD to characterize magnetic properties of metallofullerene nanopeapods, and have successfully determined the element selective magnetic moments in $Gd@C_{82}$, $(Gd@C_{82})@SWNT$, $Dy@C_{82}$, and $(Dy@C_{82})@SWNT$ the observed magnetization follows the Curie-Weiss law. The observed magnetization change between $Dy@C_{82}$ and $(Dy@C_{82})@SWNT$ indicates that encapsulation by SWNT induces charge transfer from SWNT to $Dy@C_{82}$ molecules, resulting in the change of crystal-field perturbation on Dy ions.

This work has been supported by the JST CREST Program for Novel Carbon Nanotube Materials and partially supported by the Grant-in-Aid for Scientific Research (No. 17684013). We thank T. Yamada, Y. Kitamura, T. Akachi, Y. Kato, D. Ogawa, N. Imazu, Y. Ito, Y. Asada, and H. Umemoto for assistance on SXMCD measurements in SPring-8. The SXMCD experiments were performed with the approval of JASRI [Proposal Nos. 2005B0106 (Nanotechnology Support Project) and 2005B0486].

*Corresponding author. noris@cc.nagoya-u.ac.jp

[1] H. Shinohara, Rep. Prog. Phys. **63**, 843 (2000).
[2] B. W. Smith, M. Monthioux, and D. E. Luzzi, Nature (London) **396**, 323 (1998).
[3] R. Kitaura and H. Shinohara, Chemistry An Asian Journal **1**, 646 (2006).
[4] R. Kitaura and H. Shinohara, Jpn. J. Appl. Phys., Part 1 **46**, 881 (2007).
[5] Y. Iwasa and C. J. Nuttall, Synth. Met. **135**, 773 (2003).
[6] J. Arvanitidis, K. Papagelis, S. Margadonna, K. Prassides, and A. N. Fitch, Nature (London) **425**, 599 (2003).
[7] N. Hiroshiba, K. Tanigaki, R. Kumashiro, H. Ohashi, T. Wakahara, and T. Akasaka, Chem. Phys. Lett. **400**, 235 (2004).
[8] P. Jaroenapibal, S. B. Chikkannanavar, D. E. Luzzi, and S. Evoy, J. Appl. Phys. **98**, 044301 (2005).
[9] M. A. G. Jones, J. J. L. Morton, R. A. Taylor, A. Ardavan, and G. A. D. Briggs, Physica B **243**, 3037 (2006).
[10] M. Shiraishi, S. Nakamura, T. Fukao, T. Takenobu, H. Kataura, and Y. Iwasa, Appl. Phys. Lett. **87**, 093107 (2005).
[11] B. Sitharaman, R. D. Bolskar, I. Rusakova, and L. J. Wilson, Nano Lett. **4**, 2373 (2004).
[12] B. Sitharaman, K. R. Kissell, K. B. Hartman, L. A. Tran, A. Baikalov, I. Rusakova, Y. Sun, H. A. Khant, S. J. Ludtke, W. Chiu, S. Laus, E. Toth, L. Helm, A. E. Merback, and L. J. Wilson, Chem. Commun. (Cambridge) **2005**, 3915.
[13] Y. Yasutake, Z. J. Shi, T. Okazaki, H. Shinohara, and Y. Majima, Nano Lett. **5**, 1057 (2005).
[14] J. Lee, H. Kim, S. J. Kahng, G. Kim, Y. W. Son, J. Ihm, H. Kato, Z. W. Wang, T. Okazaki, H. Shinohara, and Y. Kuk, Nature (London) **415**, 1005 (2002).
[15] H. J. Huang, S. H. Yang, and X. X. Zhang, J. Phys. Chem. B **104**, 1473 (2000).
[16] C. De Nadai, A. Mirone, S. S. Dhesi, P. Bencok, N. B. Brookes, I. Marenne, P. Rudolf, N. Tagmatarchis, H. Shinohara, and T. J. S. Dennis, Phys. Rev. B **69**, 184421 (2004).
[17] F. Bondino, C. Cepek, N. Tagmatarchis, M. Prato, H. Shinohara, and A. Goldoni, J. Phys. Chem. B **110**, 7289 (2006).
[18] K. Hirahara, K. Suenaga, S. Bandow, H. Kato, T. Okazaki, H. Shinohara, and S. Iijima, Phys. Rev. Lett. **85**, 5384 (2000).
[19] K. Suenaga, S. Iijima, H. Kato, and H. Shinohara, Phys. Rev. B **62**, 1627 (2000).
[20] S. Iida, Y. Kubozono, Y. Slovokhotov, Y. Takabayashi, T. Kanbara, T. Fukunaga, S. Fujiki, S. Emura, and S. Kashino, Chem. Phys. Lett. **338**, 21 (2001).
[21] R. D. Cowan, *The Theory of Atomic Structure and Spectra* (UCLA, Los Angles, CA, 1981).
[22] Y. M. Cho, S. W. Han, G. Kim, H. Lee, and J. Ihm, Phys. Rev. Lett. **90**, 106402 (2003).